BRAIN
A JOURNAL OF NEUROLOGY

A gradient in cortical pathology in multiple sclerosis by *in vivo* quantitative 7 T imaging

Caterina Mainero,[1,2,*] Céline Louapre,[1,2,*] Sindhuja T. Govindarajan,[1] Costanza Giannì,[1,2] A. Scott Nielsen,[2,3,4] Julien Cohen-Adad,[1,5] Jacob Sloane[2,3] and Revere P. Kinkel[2,3,6]

See Barkhof for a scientific commentary on this article (doi:10.1093/brain/awv031).
*These authors contributed equally to this work.

We used a surface-based analysis of T_2* relaxation rates at 7 T magnetic resonance imaging, which allows sampling quantitative T_2* throughout the cortical width, to map *in vivo* the spatial distribution of intracortical pathology in multiple sclerosis. Ultra-high resolution quantitative T_2* maps were obtained in 10 subjects with clinically isolated syndrome/early multiple sclerosis ($\leqslant 3$ years disease duration), 18 subjects with relapsing-remitting multiple sclerosis ($\geqslant 4$ years disease duration), 13 subjects with secondary progressive multiple sclerosis, and in 17 age-matched healthy controls. Quantitative T_2* maps were registered to anatomical cortical surfaces for sampling T_2* at 25%, 50% and 75% depth from the pial surface. Differences in laminar quantitative T_2* between each patient group and controls were assessed using general linear model ($P < 0.05$ corrected for multiple comparisons). In all 41 multiple sclerosis cases, we tested for associations between laminar quantitative T_2*, neurological disability, Multiple Sclerosis Severity Score, cortical thickness, and white matter lesions. In patients, we measured, T_2* in intracortical lesions and in the intracortical portion of leukocortical lesions visually detected on 7 T scans. Cortical lesional T_2* was compared with patients' normal-appearing cortical grey matter T_2* (paired *t*-test) and with mean cortical T_2* in controls (linear regression using age as nuisance factor). Subjects with multiple sclerosis exhibited relative to controls, independent from cortical thickness, significantly increased T_2*, consistent with cortical myelin and iron loss. In early disease, T_2* changes were focal and mainly confined at 25% depth, and in cortical sulci. In later disease stages T_2* changes involved deeper cortical laminae, multiple cortical areas and gyri. In patients, T_2* in intracortical and leukocortical lesions was increased compared with normal-appearing cortical grey matter ($P < 10^{-10}$ and $P < 10^{-7}$), and mean cortical T_2* in controls ($P < 10^{-5}$ and $P < 10^{-6}$). In secondary progressive multiple sclerosis, T_2* in normal-appearing cortical grey matter was significantly increased relative to controls ($P < 0.001$). Laminar T_2* changes may, thus, result from cortical pathology within and outside focal cortical lesions. Neurological disability and Multiple Sclerosis Severity Score correlated each with the degree of laminar quantitative T_2* changes, independently from white matter lesions, the greatest association being at 25% depth, while they did not correlate with cortical thickness and volume. These findings demonstrate a gradient in the expression of cortical pathology throughout stages of multiple sclerosis, which was associated with worse disability and provides *in vivo* evidence for the existence of a cortical pathological process driven from the pial surface.

1 A. A. Martinos Center for Biomedical Imaging, Massachusetts General Hospital, Boston, MA, USA
2 Harvard Medical School, 25 Shattuck Street, Boston, MA 02115,USA
3 Beth Israel Deaconess Medical Center, Boston, MA, USA
4 Virginia Mason Medical Center, Seattle, WA, USA
5 Institute of Biomedical Engineering, Polytechnique Montreal, Montreal, QC, Canada
6 University of California San Diego, USA

Correspondence to: Caterina Mainero, MD, PhD,
A. A. Martinos Center for Biomedical Imaging,
Massachusetts General Hospital,

Building 149, Thirteenth Street,
Charlestown,
MA 02129, USA
E-mail: caterina@nmr.mgh.harvard.edu

Introduction

Multiple sclerosis is an inflammatory demyelinating and neurodegenerative disorder of the CNS, and the leading cause of non-traumatic disability in young adults in Western countries. Histopathological examinations of multiple sclerosis brains indicate that subpial demyelinating lesions, which extend intracortically from the pia mater without reaching the white matter, are potential biomarkers of multiple sclerosis progression (Peterson *et al.*, 2001; Magliozzi *et al.*, 2010; Reynolds *et al.*, 2011).

As cortical lesions appeared topographically related to focal meningeal inflammation in some pathological studies of chronic progressive multiple sclerosis (Magliozzi *et al.*, 2007, 2010; Howell *et al.*, 2011), it has been hypothesized that cortical demyelination in multiple sclerosis may be driven by organized meningeal inflammation, accompanied by a decreasing gradient of demyelination away from the pial surface. Histopathological evidence that the cortex can be the site of inflammatory demyelinating lesions near the time of multiple sclerosis onset (Lucchinetti *et al.*, 2011) further supports the existence of an early pathological process that primarily targets the cortex, independently from white matter.

Although largely undetected on conventional MRI scans, cortical lesions, including the subpial type, have been imaged *in vivo* with improved sensitivity and spatial specificity at ultra-high field 7 T MRI (Filippi *et al.*, 2014). We previously showed that a surface-based analysis of cortical T_2^*-weighted signal from 7 T T_2^* gradient-echo images combined with a multichannel radiofrequency coil can disclose subpial T_2^* signal abnormalities in subjects with multiple sclerosis relative to healthy subjects (Cohen-Adad *et al.*, 2011), providing *in vivo* evidence for the existence of diffuse subpial pathology in multiple sclerosis, previously reported only post-mortem.

Surface-based estimation of cortical T_2^* relaxation rates provides a quantitative estimate of the biophysical changes underlying tissue integrity (Cohen-Adad *et al.*, 2012). This measure is less dependent of the technical limitations that affect measurements of T_2^*-weighted signal at ultra-high field MRI, and of potential biases that arise from cortical lesion detection based on visual inspection of scans. In the healthy brain, T_2^* relaxation time ($1/R_2^*$) inversely correlates with myelin and iron content (Langkammer *et al.*, 2010; Li *et al.*, 2011). In both white matter and cortical multiple sclerosis lesions, histopathological–magnetic resonance correlations showed that demyelination and iron loss induce an increase in T_2^* relaxation time (Yao *et al.*, 2012, 2014), whereas iron accumulation relates to shorter T_2^* (Bagnato *et al.*, 2011).

We demonstrated that surface-based mapping of quantitative T_2^* as a function of cortical depth (laminar analysis) from ultra-high resolution gradient echo 7 T MRI images is highly reproducible (Govindarajan *et al.*, 2015) and could prove useful for studying the myelo-architecture of the cortex *in vivo* (Cohen-Adad *et al.*, 2012), and for characterizing conditions associated with changes in cortical myelin and/or iron concentration.

In this study, we used a surface-based laminar analysis of 7 T quantitative T_2^* to test the following hypotheses: (i) cortical pathology in multiple sclerosis is associated with changes in quantitative T_2^*, which differ across disease stages: quantitative T_2^* abnormalities mainly involve the outer cortical layers and sulci in early disease; while they can also be detected in deeper cortical layers and gyri in later stages and progressive multiple sclerosis; and (ii) neurological disability and multiple sclerosis severity correlate with the degree of laminar quantitative T_2^* abnormalities. A further aim was to investigate the contribution of cortical laminar pathology, as measured by quantitative T_2^*, to cortical thinning in multiple sclerosis. Finally, we measured quantitative T_2^* in multiple sclerosis cortical lesions, detected visually on 7 T scans, as well as in normal-appearing cortical grey matter (NACGM), to better understand their role in determining laminar quantitative T_2^* changes in multiple sclerosis.

Materials and methods

Subjects

Forty-one patients [29 females; mean age = 43.2 ± 8.8 standard deviation (SD) years] were prospectively included in the study. Eligibility criteria were: age between 18 and 60 years, a diagnosis of clinically isolated syndrome or multiple sclerosis (McDonald *et al.*, 2001). Patients were enrolled according to three disease phenotypic categories: (i) clinically isolated syndrome - early multiple sclerosis ($n = 10$): $\leqslant 3$ years disease duration; (ii) relapsing remitting multiple sclerosis (RRMS, $n = 18$) with $\geqslant 4$ years disease duration; and (iii) secondary progressive multiple sclerosis (SPMS, $n = 13$) (Lublin and Reingold, 1996).

Exclusion criteria for multiple sclerosis subjects included a clinical relapse within 3 months of enrolment, corticosteroid therapy within 1 month of scanning, and other neurologic and/ or significant psychiatric disease. Neurological disability in patients was assessed using the Expanded Disability Status Scale (EDSS) (Kurtzke, 1983). The Multiple Sclerosis Severity Score (MSSS) was calculated on each patient using their EDSS and duration from onset of multiple sclerosis symptoms, as previously detailed (Roxburgh *et al.*, 2005). Thirty-three of 41 patients were on treatment with disease-modifying agents for at least 6 months, while the remaining eight subjects were not receiving any therapy for multiple sclerosis.

Seventeen age-matched healthy volunteers (nine females; mean age = 39.3 ± 8.8 SD years) served as controls. General exclusion criteria included significant psychiatric and/or neurological disease (other than multiple sclerosis for patients), major medical comorbidity, pregnancy, and contraindications for MRI.

Subjects gave their written informed consent to participate in the study and the local Ethics Committee of our Institution approved the study procedures.

MRI data acquisition

All subjects underwent, on a 7 T Siemens whole-body scanner using a custom-built 32-channel phased array coil, acquisition of: (i) multi-echo 2D FLASH T_2*-weighted spoiled gradient-echo imaging, repetition time = 2210 ms, echo time = $6.44 + 3.32$ n $[n = 0, \ldots, 11]$ ms, flip angle = 55°, two slabs of 40 slices each to cover the supratentorial brain, field of view = 192×168 mm², resolution = $0.33 \times 0.33 \times 1$ mm³ (25% gap), bandwidth = 335 Hz/pixel, acquisition time for each slab = ~10 min; (ii) a T_1-weighted 3D magnetization-prepared rapid acquisition gradient echo sequence (MPRAGE, repetition time/inversion time/echo time = 2600/1100/3.26 ms, flip angle = 9°, field of view = 174×192 mm², resolution = $0.60 \times 0.60 \times 1.5$ mm³, bandwidth = 200 Hz/ pixel, acquisition time = 5.5 min) for co-registration of 7 T gradient-echo data with cortical surfaces; and (iii) a single-echo 2D FLASH T_2*-weighted spoiled gradient-echo pulse sequence (repetition time/echo time = 1700/21.8 ms, the other parameters being identical to the multi-echo 2D FLASH T_2* sequence).

In addition to the 7 T session, all subjects were scanned once on a 3 T Siemens scanner (Tim Trio) using the Siemens 32-channel coil to acquire a structural scan with a 3D magnetization-prepared rapid acquisition with multiple gradient echoes (MEMPR) [repetition time/inversion time = 2530/1200 ms, echo time = (1.7, 3.6, 5.4, 7.3) ms, flip angle = 7°, field of view = 230×230 mm², resolution = $0.9 \times 0.9 \times 0.9$ mm³, bandwidth = 651 Hz/pixel, acquisition time = ~6.5 min] for cortical surface reconstruction, co-registration with 7 T data, and cortical thickness and cortical volume estimation.

MRI data processing

White matter lesion volume

White matter lesion volume (mm³) was assessed from white matter lesions segmented on magnitude images from 7 T single-echo FLASH T_2* scans using a semi-automated method implemented in 3D Slicer version 4.2.0 (http://www.slicer.org).

Cortical surface reconstruction, cortical thickness and volume estimation

Pial and white matter surfaces, cortical thickness maps, and cortical volumes were obtained using the software FreeSurfer, version 5.3.0 (http://surfer.nmr.mgh.harvard.edu/), according to a multi-step procedure that calculates the grey matter/ white matter border and the CSF/grey matter (pial) border in the 3D MEMPR volume (Dale *et al.*, 1999). Topological defects in cortical surfaces due to white matter and leukocortical lesions were corrected using a semi-automated procedure with lesions filling.

Mean cortical thickness was measured in each subject as the distance (mm) between the grey matter/white matter boundary and the pial surface (Fischl and Dale, 2000). For each subject, we also estimated the mean normalized cortical volume defined as the ratio between mean cortical volume and total intracranial volume as assessed in Freesurfer.

For vertex-by-vertex surface-based cortical thickness analyses across subjects' groups, each individual subject's surface was smoothed using a 10 mm full-width at half-maximum Gaussian kernel, and subsequently registered to a surface template 'fsaverage' using FreeSurfer.

Quantitative T_2* mapping along the cortex

T_2* signal was corrected at each voxel for susceptibility-induced through-slice dephasing as described previously (Cohen-Adad *et al.*, 2012). A Levenberg–Marquardt nonlinear regression model was then used to fit voxel-wise the corrected T_2* signal versus echo time; R^2 goodness of fit was measured, and voxels with poor fit ($R^2 < 0.8$) were excluded from further analyses. Poor fits were typically present in lower brain regions including the temporal pole, and in regions at the tissue/air interface (close to the sinuses).

Each individual T_2* map was registered to the corresponding 3 T cortical surface using a boundary-based registration algorithm (Greve and Fischl, 2009), as previously detailed (Cohen-Adad *et al.*, 2012). The registered T_2* data were concatenated into a whole brain volume using Freesurfer tools and resampled at 0.33 mm³ isotropic resolution.

T_2* was sampled along the entire cortex in right and left hemispheres at 25%, 50% and 75% depth from the pial surface (0% depth) towards grey matter/white matter boundary (100% depth) over the surface of each individual subject, and smoothed along the cortical surface using a 5 mm full-width at half-maximum Gaussian kernel. Given that cortical thickness varies throughout the cortex, depth was not defined as an absolute distance between the pial and the grey matter/white matter boundary, but rather as a relative distance between the pial and white matter surface. We used an equidistant model for sampling quantitative T_2* within the cortex as it has shown excellent reproducibility (Govindarajan *et al.*, 2015), and has been found comparable to equivolume modelling when investigating *in vivo* data with spatial resolution similar to those used in our study (Waehnert *et al.*, 2014).

Because it is unclear whether leukocortical lesions, which extend across cortex and white matter but do not reach the pial surface, originate from cortex or white matter, such lesions were not masked in quantitative T_2* maps.

For group analyses, all subjects' surfaces were then registered to the surface template 'fsaverage' using FreeSurfer.

Quantitative T_2* in focal cortical lesions

Using Slicer, two raters, blinded to patients' demographic and clinical data, segmented by consensus, on magnitude images from 7 T single-echo FLASH T_2*, focal cortical multiple sclerosis lesions that appeared as focal cortical hyperintensities extending for at least three voxels and across two consecutive slices. In subjects with multiple sclerosis, focal cortical lesions were characterized as (i) intracortical lesions including lesions originating from the pial surface and extending at different depths throughout the cortical width (type III-IV lesions), and type II lesions (Peterson *et al.*, 2001; Bo *et al.*, 2003b); and (ii) leukocortical lesions extending through grey matter/white matter without reaching the pial surface. Areas of NACGM were also identified in each multiple sclerosis subject throughout the cortex.

Subsequently, in each subject, intracortical lesions, leukocortical lesions and NACGM masks were created and coregistered, using a boundary-based registration method (Greve and Fischl, 2009), to the corresponding cortical quantitative T_2* maps for estimating mean quantitative T_2* (ms) in each mask. Given that the focus of the study was the cortex, for leukocortical lesions quantitative T_2* was measured only in the intracortical portion of the mask.

Statistical methods

A general linear model (GLM) was run on a vertex-by-vertex basis across the whole cortex, using Freesurfer tools, to assess: (i) differences in quantitative T_2* at each depth from the pial surface (25%, 50%, 75%) between controls and the three subgroups of patients (early multiple sclerosis, RRMS, SPMS); (ii) the relationship, in all patients, between quantitative T_2* at 25%, 50% and 75% depth and EDSS and MSSS; (iii) cortical thickness differences between patients and controls; and (iv) the relationship between quantitative T_2* at each depth and cortical thickness across the whole cortex using the per-vertex regressor option in Freesurfer, which allows testing at the vertex level for possible correlations between two imaging modalities. Age was used as a nuisance factor (covariate of no interest) in all GLM analyses.

For all surface-based group analyses we performed a clusterwise correction for multiple comparisons using a Monte-Carlo simulation with 10 000 iterations (Hagler *et al.*, 2006). Localization of significant clusters across the cortex was performed using the Desikan atlas in Freesurfer.

For comparisons of conventional MRI metrics (whole mean cortical thickness, normalized cortical volume, and white matter lesion volume) across patients' groups relative to controls and correlations with clinical variables, analysis of covariance (ANCOVA) controlled for age, and Spearman rank correlation coefficient were performed using the software R (version 2.13.1). In patients, differences between mean quantitative T_2* in intracortical lesions, and leukocortical lesions relative to mean quantitative T_2* in NACGM were assessed using paired *t*-test; differences between mean quantitative T_2* in intracortical lesions, leukocortical lesions, NACGM in patients and mean cortical quantitative T_2* in healthy subjects were assessed using linear regression using age as covariate of no interest (R software, version 2.13.1). For all analyses, statistically significant threshold was set at *P*-value < 0.05

Sulci and gyri analysis

Using the Freesurfer masks of gyri and sulci, we assessed whether quantitative T_2* changes in patients preferentially involved cortical sulci or cortical gyri. The masks of gyri and sulci were applied to all clusters that exhibited significant differences in quantitative T_2* at the GLM (corrected $P < 0.05$) in each patient subgroup (early multiple sclerosis, RRMS, SPMS) relative to controls, at each depth (25%, 50%, 75%). In each mask the surface area (mm^2) of vertices exhibiting significant quantitative T_2* changes was computed. For comparison, given that the surface area of sulci is ~14% smaller than the surface area of gyri, the surface areas (mm^2) of significant quantitative T_2* changes in sulci and gyri were normalized by the total cortical surface area.

Results

Participants' demographics, including EDSS and MSSS in patients, and conventional MRI metrics are reported in Table 1.

Laminar quantitative T_2* in multiple sclerosis across the cortex

Figure 1 and Supplementary Table 1 illustrate the results of the GLM laminar analysis comparing 7 T quantitative T_2* at 25%, 50% and 75% depth from the pial surface in the earliest disease stages, RRMS and SPMS relative to healthy subjects, and the overlap of significant clusters across the three patients' groups. In all subgroups of patients we observed, relative to controls and in both hemispheres, a significant increase in T_2* relaxation time (clusterwise $P < 0.05$, corrected for multiple comparisons), consistent with myelin and iron loss. Scattered small clusters of shorter quantitative T_2*, suggestive of increased susceptibility effects and/or increased iron content, were seen in each disease group mainly in frontal and temporal areas (Supplementary Table 1).

In early multiple sclerosis, significant clusters of longer T_2* were mainly located in the outer cortical layers, at 25% depth from the pial surface, in the rostral anterior cingulate and parietal regions, as well as in the precentral and postcentral cortex. Fewer clusters of longer T_2* were present in deeper cortical laminae, specifically in the postcentral, and occipital cortex at 50% depth, whereas there was only one cluster of increased quantitative T_2* in the calcarine cortex at 75% depth (Supplementary Table 1). Subjects with RRMS and longer disease duration showed a discrete involvement of all cortical layers across frontal, parietal, occipital regions, as well as in the isthmus cingulate and temporal cortex (Supplementary Table 1). Subjects with SPMS showed diffuse cortical involvement at all depths throughout the cortical mantle (Supplementary Table 1).

Table 1 Demographic and conventional MRI characteristics of study subjects

	Controls	MS patients	Early MS	Late RRMS	SPMS
n	17	41	10	18	13
Gender (M/F)	8/9	12/29	2/8	5/13	5/8
Age, years mean (SD)	39.3 (8.8)	43.2 (8.8)	38.3 (10.5)	44.3 (7.6)	45.5 (8.1)
Disease duration, years, mean (SD)	–	11.5 (8.0)	2.8 (1.1)	11.4 (4.3)	18.5 (8.4)
EDSS score, mean (SD)	–	3.3 (1.8)	2.2 (0.8)	2.5 (1.2)	5.2 (1.6)
MSSS, mean (SD)	–	4.3 (2.4)	5.0 (1.8)	2.9 (2.0)	5.5 (2.4)
CT, mm mean (SD)	2.5 (0.09)	2.40 (0.11)[a]	2.43 (0.09)	2.42 (0.10)	2.35 (0.14)[b]
NCV, mean (SD)	0.33 (0.06)	0.29 (0.02)[c]	0.30 (0.02)	0.29 (0.02)[d]	0.28 (0.03)[e]
WMLV, cm^3 mean (SD)	–	5.7 (9.1)	1.7 (2.2)	2.5 (2.4)	13.4 (13.3)
ICL, *n* median (range)	–	6 (0–55)	5 (0–22)	4.5 (0–23)	30 (2–55)
LCL, *n* median (range)	–	3 (0–137)	0.5 (0–18)	1.5 (0–18)	37 (0–137)

MS = multiple sclerosis; CT = cortical thickness; NCV = normalized cortical volume; ICL = intracortical lesions; LCL = leukocortical lesions; WMLV = white matter lesion volume.
[a] $P < 0.02$ = all multiple sclerosis versus controls; [b] $P < 0.02$ = SPMS versus controls; [c] $P < 0.005$ = all multiple sclerosis versus controls; [d] $P = 0.08$, RRMS versus controls; [e] $P = 0.07$, SPMS versus controls, by ANCOVA.
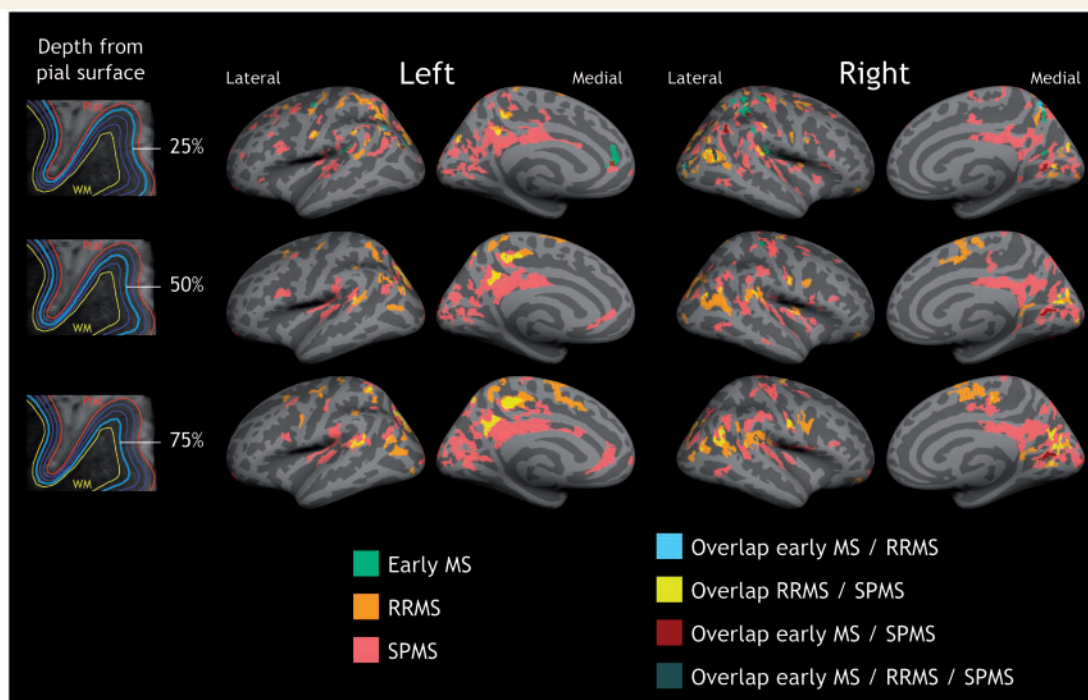

Figure 1 Quantitative T$_2$* differences between multiple sclerosis patients and controls. Overlay of the GLM significance maps ($P < 0.05$ corrected for multiple comparisons) on the average pial surface showing in the three subgroups of patients, early multiple sclerosis (MS), RRMS and SPMS, clusters of increased T$_2$* relaxation time relative to healthy controls at 25% (*top row*), 50% (*middle row*), and 75% depth (*bottom row*) from the pial surface, as well as overlap of significant clusters across patients' subgroups. In early disease, quantitative T$_2$* changes were focal and mainly confined to the juxtameningeal cortex, and cortical sulci (darker grey areas); in RRMS and SPMS quantitative T$_2$* changes involved deeper cortical laminae, and multiple cortical areas. WM = white matter.

In patients, the surface area of increased quantitative T$_2$* relative to controls (normalized by the total cortical surface area) was greater in cortical sulci than in gyri, across all cortical depths in early multiple sclerosis and SPMS, and at 25% depth in RRMS (Fig. 2). The greater involvement of cortical sulci relative to gyri was prominent in early disease.

Quantitative T$_2$* in focal cortical lesions and normal-appearing cortical grey matter

Cortical lesions counts in all multiple sclerosis subjects and in each multiple sclerosis subgroup are shown in Table 1.
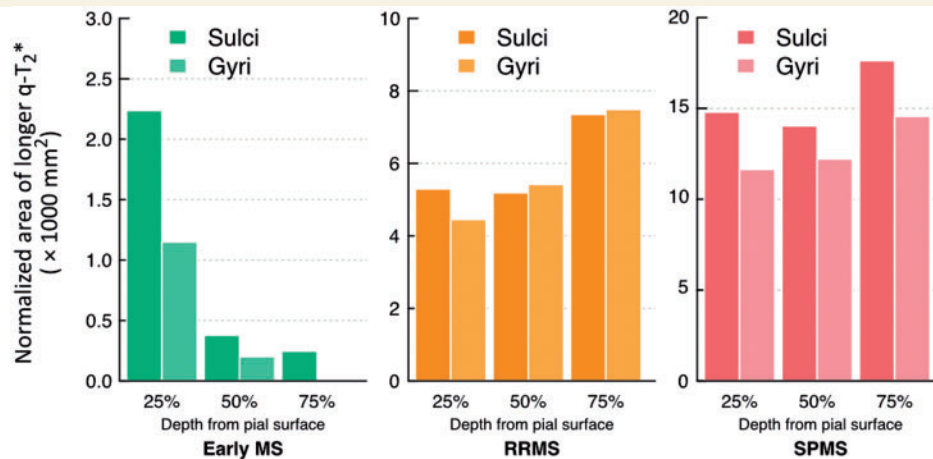
Figure 2 Distribution of T_2* changes in patients in cortical sulci and gyri. Diagram illustrating the distribution of vertices exhibiting increased T_2* relaxation time in subjects with early multiple sclerosis, RRMS and SPMS, relative to controls, at 25%, 50% and 75% depth from the pial surface, across cortical sulci and cortical gyri, and expressed as the total surface area (mm^2) in significant sulcal or gyri vertices normalized by the total cortical surface area. q-T_2* = quantitative T_2*.

In all patients, mean quantitative T_2* in intracortical lesions (40.2 ± 5.1 ms) and leukocortical lesions (40.1 ± 4.7 ms) was significantly higher than mean NACGM quantitative T_2*(33.5 ± 2.5 ms) ($P < 10^{-10}$ and $P < 10^{-7}$ by paired *t*-test), and than mean cortical quantitative T_2* (33.03 ± 1.6 ms) in controls ($P < 10^{-5}$ and $P < 10^{-6}$ by linear regression). This comparison remained significant in each multiple sclerosis subgroup (Supplementary Table 2). Although there were no significant differences between NACGM quantitative T_2* in all patients and mean cortical quantitative T_2* in controls, NACGM quantitative T_2* in SPMS cases was significantly increased relative to cortical quantitative T_2* from healthy subjects (Supplementary Table 2).

Cortical thickness and laminar quantitative T_2*

Overall, patients ($n = 41$) showed significantly decreased mean cortical thickness and normalized cortical volume (ie. entire cortex) relative to healthy subjects ($P < 0.02$ and $P < 0.005$ by ANCOVA, Table 1). Significant cortical thinning was also observed in SPMS subjects ($P < 0.02$ by ANCOVA, Table 1), and there was a trend towards significance for decreased normalized cortical volume in the RRMS and SPMS subgroups ($P < 0.08$ and $P < 0.07$ by ANCOVA, Table 1). The observed decrease in mean global cortical thickness and normalized cortical volume in the entire multiple sclerosis group ($n = 41$) relative to controls was not exclusively driven by SPMS subjects, as we also observed significant cortical thinning and cortical volume loss in early multiple sclerosis and RRMS when grouped together ($P < 0.02$ and $P < 0.05$ by ANCOVA, data not shown).

The GLM analysis between patients and controls did not disclose significant regional changes in cortical thickness after correction for multiple comparisons. We found that in patients, in several regions of both hemispheres, thinning of the cortex corresponded to longer T_2* ($P < 0.05$ corrected) at all three depths from the pial surface (Fig. 3 and Table 2). Because of the negative correlation in subjects with multiple sclerosis between laminar quantitative T_2* and cortical thickness across several cortical areas, we assessed differences in laminar quantitative T_2* (25%, 50% and 75% depth) between each patients' subgroup and controls using a GLM with per-vertex regression of cortical thickness as a covariate of no interest (nuisance factor), along with age. Increase in quantitative T_2* across disease stages and depths remained significant ($P < 0.05$ corrected) and substantially unchanged after regressing out cortical thickness (Fig. 4).

Correlation with clinical measures

We did not find any relation between either regional or global cortical thickness and normalized cortical volume and either EDSS or MSSS, whereas white matter lesion volume was positively associated with EDSS ($P < 0.008$ by Spearman test) but not with MSSS.

Figure 5 shows the results of the GLM analysis investigating the relationship between both EDSS and MSSS in all patients and laminar quantitative T_2* at all three depths (25%, 50%, 75%) from the pial surface. There was a positive correlation ($P < 0.05$ corrected) between quantitative T_2* and both EDSS and MSSS at all depths, the greatest association being observed at 25% depth from the pial surface for both EDSS and MSSS (Table 3). Across all cortical depths, clusters showing a significant correlation between quantitative T_2* and EDSS and MSSS were mostly
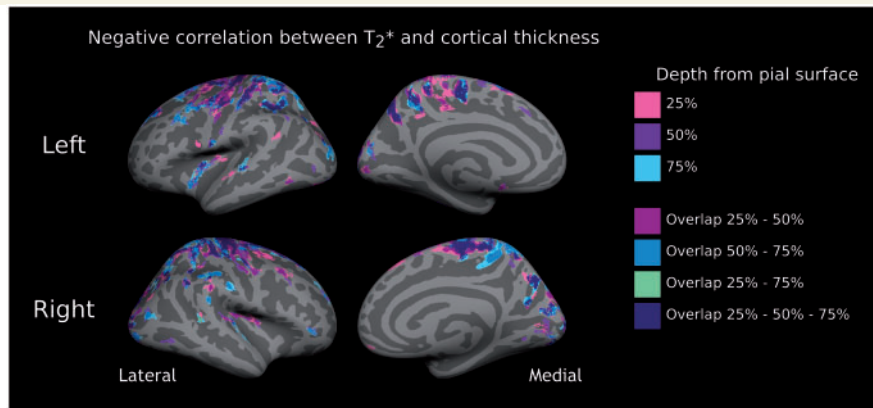
Figure 3 Relationship between laminar T_2^* and cortical thickness in patients. Overlay of the GLM significance maps ($P < 0.05$ corrected for multiple comparisons) on the average pial surface for left (*top*) and right (*bottom*) hemispheres showing, in the whole group of subjects with multiple sclerosis ($n = 41$), clusters exhibiting a negative correlation between T_2^* relaxation time at 25%, 50% and 75% depth from the pial surface and cortical thickness, as well as significant clusters overlapping across the three depths.

Table 2 Location of clusters exhibiting a significant negative correlation ($P < 0.05$, corrected) between 7 T T_2^* relaxation time at 25%, 50% and 75% depth from the pial surface and cortical thickness in 41 subjects with multiple sclerosis

	Left hemisphere	Right hemisphere
T_2^* 25%	Medial orbitofrontal - caudal middle frontal - superior frontal	Medial orbitofrontal - caudal middle frontal - superior frontal
	Precentral - postcentral	Paracentral - precentral - postcentral
	Insula - superior temporal - inferior temporal	Superior temporal - bankssts
	Superior parietal - inferior parietal - supramarginal - precuneus - posterior cingulate	Superior parietal - inferior parietal
	Lateral occipital - cuneus - fusiform	Supramarginal - precuneus
		Lateral occipital - cuneus - pericalcarine - lingual
T_2^* 50%	Medial orbitofrontal - caudal middle frontal - superior frontal	Pars triangularis - rostral middle frontal
	Paracentral - precentral - postcentral	Caudal middle frontal
	Insula - superior temporal - inferior temporal	Paracentral
	Superior parietal - inferior parietal	Insula - superior temporal - transverse temporal
	Supramarginal - precuneus	Superior parietal - inferior parietal - supramarginal - precuneus
	Lateral occipital - cuneus - lingual	Lateral occipital - pericalcarine - lingual
T_2^* 75%	Caudal middle frontal - superior frontal	Pars triangularis - rostral middle frontal
	Paracentral - precentral - postcentral	Superior frontal
	Insula - superior temporal - inferior temporal	Precentral - postcentral
	Superior parietal - inferior parietal - supramarginal	Superior temporal - bankssts
	Precuneus - cuneus - lateral occipital	Superior parietal - inferior parietal - supramarginal - precuneus
		Lateral occipital - cuneus

Bankssts = banks of the superior temporal sulcus.

located in the sensorimotor cortex, though other significant clusters were observed in the insula, cingulate, prefrontal, parietal, and temporal cortex, and this was mainly observed at 25% depth. The significant association between EDSS and laminar quantitative T_2^* remained significant after including in the GLM analysis, in addition to age, white matter lesion volume as a nuisance variable (covariate of no interest) (Fig. 5 and Table 3).

Discussion

Subpial lesions are thought to constitute a major pathological substrate for disease progression in multiple sclerosis. Ultra-high field MRI enables improved detection and classification of focal cortical lesions in multiple sclerosis relative to lower field ($\leqslant 3$ T) MRI (Filippi *et al.*, 2014), but *in vivo* quantification of disseminated subpial
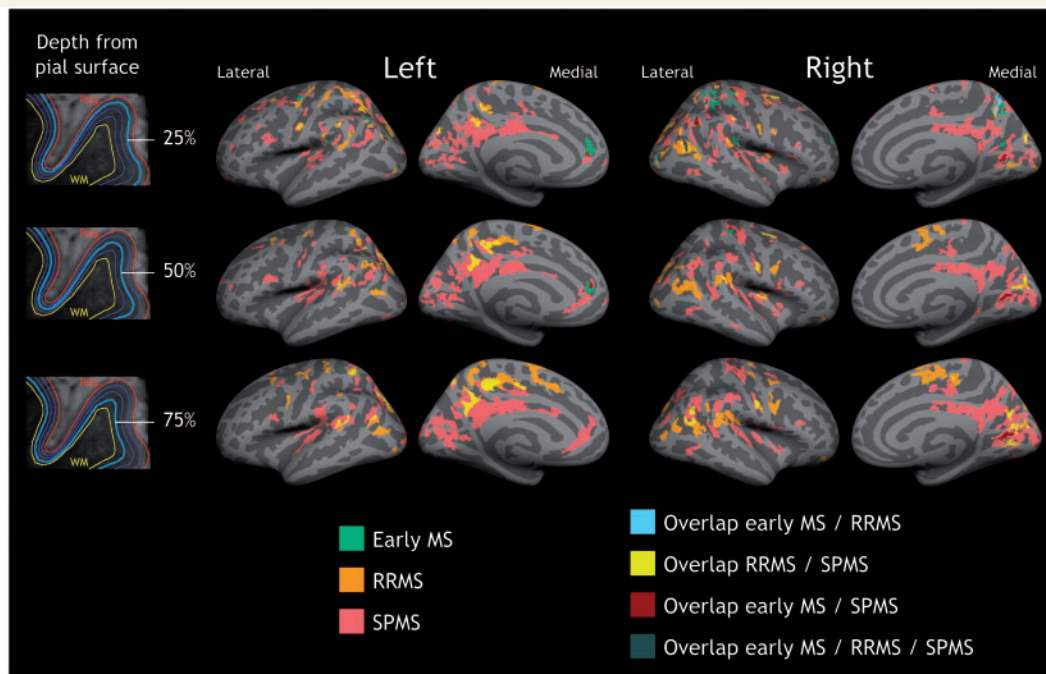
Figure 4 Quantitative T$_2$* differences between multiple sclerosis patients and controls independent from cortical thickness. Overlay of the GLM significance maps ($P < 0.05$ corrected for multiple comparisons) on the average pial surface showing in early multiple sclerosis (MS), RRMS and SPMS, clusters of increased T$_2$* relaxation time relative to healthy controls at 25%, 50% and 75% depth from the pial surface, after including in the GLM cortical thickness at the vertex level as a covariate of no interest, along with age. WM = white matter.
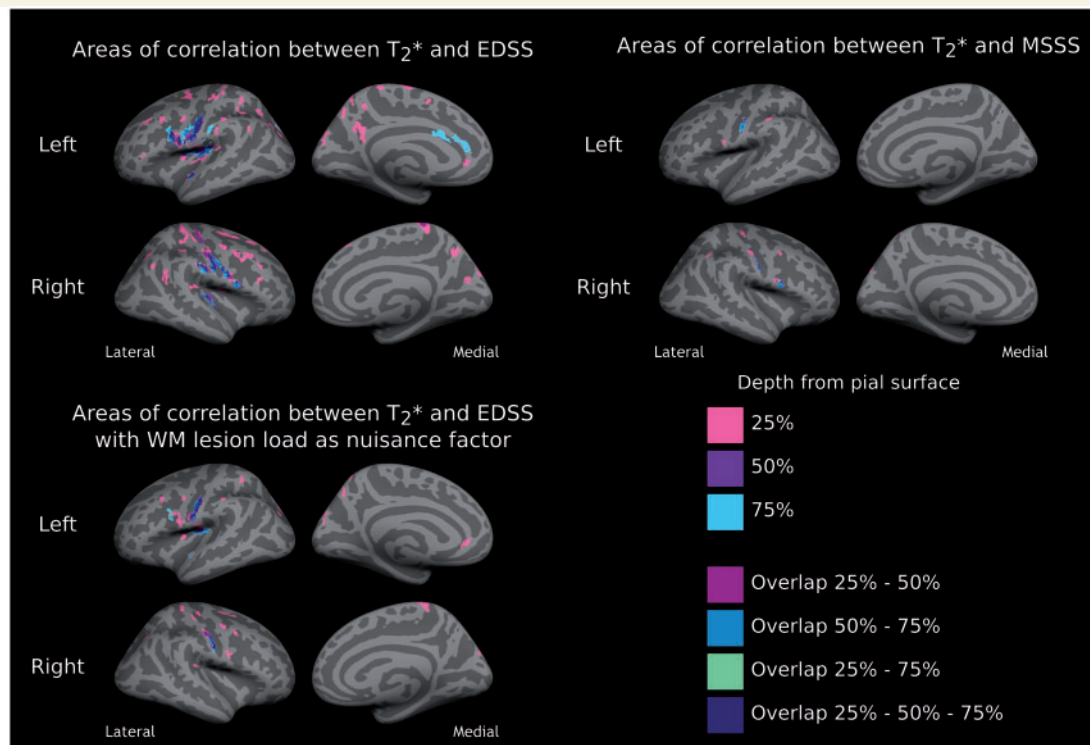

Figure 5 Relationship between quantitative T$_2$*, disability and disease severity. Overlay of the GLM significance maps ($P < 0.05$ corrected for multiple comparisons) showing in 41 subjects with multiple sclerosis clusters exhibiting a positive correlation between T$_2$* relaxation time at 25%, 50% and 75% depth from the pial surface and neurological disability, as measured by EDSS, and disease severity, as measured by the MSSS. Overlaid are also significant clusters overlapping across the three depths. The positive correlation between EDSS and quantitative T$_2$* remained significant even after including white matter (WM) lesion load as a covariate of no interest (nuisance variable) in the GLM (*bottom*).

Table 3 Clusters of significant positive correlation between quantitative T_2^* at 25%, 50% and 75% depth from the pial surface and EDSS and MSSS in 41 subjects with multiple sclerosis

	EDSS score						MSSS score					
	25%		50%		75%		25%		50%		75%	
	P-value	S-area (mm²)	P-value	S-area (mm²)	P-value	S-area (mm²)	P-value	S-area (mm²)	P-value	S-area (mm²)	P-value	S-area (mm²)
LEFT HEMISPHERE												
Pars triangularis	0.02	38.98										
Rostral middle frontal	0.0001	88.57										
Caudal middle frontal	0.0001	80.6										
Superior frontal	0.02	39.31										
Rostral ant. cingulate	0.04	35.45			0.0001	132.58						
Caudal ant. cingulate					0.009	89.31						
Precentral	**0.0001** **0.0006**	**996.28** **58.57**	**0.0001**	**227.7**	**0.0001**	**152.53**	0.03	37.93				
Post central	**0.0001**	**730.19**	**0.0001**	**584.04**	**0.0001** 0.009	**700.09** 89.4	0.03	37.77	0.0007	120.31	0.0001	156.88
Paracentral	0.0002 0.0001	67.12 103.84										
Superior parietal	**0.0001** 0.04	**618.05** 36.18			0.01	84.31	0.0005 0.03	63.87 37.44				
Supramarginal	0.001 0.01 0.0001	54.58 43.41 84.86			0.05	69.84	0.004	48.98				
Inferior parietal	0.004 0.01 0.0001	48.71 41.9 160.57										
Superior temporal	0.0001 0.006	96.99 46.06	0.01	87.22	**0.004**	**98.12**						
Insula	**0.0001**	**70.27**	**0.0001**	**722.81**	**0.0001**	**764.52**						
Precuneus	0.0001 0.02	548.42 77.54										
RIGHT HEMISPHERE												
Pars opercularis			0.002	105.49	0.002	105.81			0.03	73.99		
Rostral middle frontal	0.008 0.01	45.02 43.86										
Caudal middle frontal	**0.0001**	**281.48**					0.04	36.16				
Superior frontal	**0.004** 0.0002 0.009 0.0001	**47.7** 66.55 43.77 83.62										
Precentral	**0.0001** 0.02 0.0002	**506.47** 40.1 66.39			0.0001	197.61	0.001 0.003	53.33 49.99			0.01	84.02
Post central	**0.003** **0.0001**	**50.36** **576.83**	**0.0001** 0.0002	**620.82** 131.78	**0.0001**	**256.13**	0.05 0.0001	35.66 74.65	0.005	95.68	0.01	80.4
Paracentral	**0.0001**	**172.44**	0.05	69.9								
Supramarginal	0.0007 0.0001	115.2 102.32	0.0005	119.69	0.0004	121.36						
Inferior parietal	**0.0001** 0.001	**225.63** 56.19					0.02	39.43				
Insula			0.0001	181.95								
Superior temporal	**0.02**	**40.87**			0.0003	126.94						
Transverse temporal	0.003	51.14										
Precuneus	0.0002	225.82										
Cuneus	**0.0001**	**226.37**										

Clusters in bold represent clusters that remained significant after including in the GLM white matter lesions as a nuisance factor (covariate of no interest).
S-area = surface area; ant = anterior.

demyelination remains challenging. In this study, using a surface-based technique on ultra-high resolution 7 T quantitative T_2* maps ($\sim$0.13 mm^3 voxel size), we demonstrated *in vivo* the presence of pathological changes that involve predominantly the outer layers of the cerebral cortex and cortical sulci in the earliest stages of multiple sclerosis, and extend to deeper cortical laminae and gyri in later disease, becoming diffuse across the whole cortical width and mantle in SPMS.

Comparative post-mortem MRI and histopathology data suggested that conventional imaging methods are not able to reliably detect cortical disease cases in which pathology is confined to the juxtameningeal cortex, based on the observation that visibility of multiple sclerosis cortical lesions at lower strength field MRI depended uniquely on lesions size and involvement of several cortical layers (Seewann et al., 2011). The surface-based technique that allows quantitative T_2* at 7 T to be estimated vertex-wise across the whole cortical mantle and width could, thus, prove to be a powerful alternative imaging tool for assessing *in vivo* juxtameningeal cortical pathology in such multiple sclerosis cases.

Histopathological studies suggested that all brain lobes can be the site of cortical lesions, although some pathological findings reported a preferential distribution of cortical demyelination in the insula, cingulate and the temporobasal cortex (Bo et al., 2003b; Kutzelnigg and Lassmann, 2006). In our multiple sclerosis cohort, changes in cortical quantitative T_2*, particularly in SPMS, were distributed across the cortical mantle. Frontal, sensorimotor and parietal areas seemed to be preferred sites of pathological changes at all disease stages.

Quantitative T_2* changes in cortical sulci and gyri

There is evidence that the histopathological and immunological characteristics of subpial demyelination differ significantly from those in white matter lesions, which suggests a location-dependent expression of the multiple sclerosis immunopathological process (Peterson et al., 2001; Bo et al., 2003a, 2007). Autopsy studies of progressive multiple sclerosis showed that more aggressive subpial pathology was associated with the presence of ectopic meningeal B cell follicular-like structures that were located along and in the depth of the cerebral sulci (Magliozzi et al., 2007, 2010; Howell et al., 2011), and which are thought to trigger cortical demyelination through the activation of microglia (Lassmann and Lucchinetti, 2008). The role of ectopic meningeal B cell follicles in early multiple sclerosis has not been elucidated yet, and, in general, evidence of meningeal inflammation in the early stage of multiple sclerosis is limited. Biopsies on atypical multiple sclerosis cases at disease onset described meningeal inflammation by means of perivascular cells infiltration, in association with cortical demyelinating lesions (Lucchinetti

et al., 2011). *In vivo* studies assessing at lower field strength MRI magnetization transfer imaging (MTR) in the cortex of patients with multiple sclerosis failed to observe a disease effect on cerebral sulci (Samson et al., 2013), possibly due to partial volume effects between the cortex and adjacent white matter and CSF (1 mm^3 voxel size). The authors, however, were able to detect global changes in MTR in the outer portion of the cortex in RRMS and SPMS patients relative to healthy subjects (Samson et al., 2014). Other findings using a surface-based analysis on MTR images at 1.5 T found decreased MTR in the mid-cortical surface (50% depth from the pial surface) in a small cohort of multiple sclerosis subjects relative to healthy controls, however, a quantitative assessment of MTR differences across cortical layers and in sulci versus gyri was not performed (Derakhshan et al., 2014). We found that, in early disease and in SPMS across all cortical depths and in RRMS at 25% depth, quantitative T_2* changes preferentially involved cortical sulci rather than cortical gyri, corroborating the hypothesis that subpial demeylination is a process likely facilitated by the adjacent meningeal inflammatory milieu. The preferential localization of subpial demyelination in cortical sulci could be related to the tendency of meningeal inflammatory cells and soluble mediators to collect and concentrate in sulci, while being diluted at the outer gyral brain surface due to physiological flow variations of CSF. As disease progresses, persistence of inflammatory changes, and lack of effective repair mechanisms can induce further demyelination that spreads to cortical gyri leading to the phenomenon termed 'general subpial demyelination' (Bo et al., 2003b), described in late stage multiple sclerosis. Interestingly, in our study, involvement of cerebral sulci was prominent in early multiple sclerosis, whereas involvement of cortical gyri increased in later disease stages.

Cortical quantitative T_2* and clinical measures

Post-mortem studies in chronic progressive multiple sclerosis demonstrated an association between a decreasing gradient of intracortical demyelination and neuronal loss away from the pial surface and disease severity as measured by age at which patients became wheelchair-dependent (Magliozzi et al., 2007, 2010).

We previously reported in different multiple sclerosis cohorts an association between neurological disability and the number of focal subpial lesions on 7 T T_2*-weighted images, which also included type IV cortical lesions that extend from the pial surface through the entire cortical width without reaching the subcortical white matter (Mainero et al., 2009; Nielsen et al., 2013). Here, the laminar analysis of quantitative T_2* revealed a significant positive relation between T_2* relaxation time at all three cortical depths (25%, 50%, 75%) and both EDSS and MSSS, the greatest effect being in the outer cortical layers

(25% depth). This association was independent of underlying white matter lesions, indicating that subpial pathology has a significant and unique contribution to disability and disease severity in multiple sclerosis.

The greatest association in our multiple sclerosis cohort between EDSS and MSSS and quantitative T_2^* at 25% depth is in line with neuropathological examinations that observed that multiple sclerosis brains with a decreasing gradient of demyelination and neuronal loss away from pial surface (likely linked to meningeal inflammation) could be distinguished from other multiple sclerosis cases that lacked a gradient in the expression of cortical pathology, despite the presence of neuronal loss and translaminar cortical demyelination (Magliozzi *et al.*, 2010). Clinically, these patients exhibited a milder disease course compared to the former group suggesting that a pathogenic mechanism for cortical demyelination driven from the cortical surface, and possibly associated with meningeal inflammation, is related with worse clinical outcome.

In our early multiple sclerosis cohort, cortical quantitative T_2^* changes were mainly found in the outer portion of the cortex. Interestingly, early patients showed levels of neurological disability similar to subjects with late RRMS. This, given the short disease duration, translated into higher MSSS, thus implying the presence of a clinically aggressive early disease course. It is also possible that some patients with a relatively benign disease course have been included in the late RRMS group. The term 'benign', however, is still controversial as the course of multiple sclerosis can worsen at any time, even after many years of apparent stability (Lublin, 2014), and frequently does not take into account cognitive deficits that may occur in multiple sclerosis in the presence of mild physical disability. Indeed our data demonstrate the presence of distributed cortical quantitative T_2^* at different depths from the pial surface in the RRMS group relative to healthy individuals. Longitudinal evaluations are needed to better elucidate the role of intracortical quantitative T_2^* to disease progression and cognitive impairment in multiple sclerosis.

Cortical quantitative T_2^* and cortical thickness

We investigated the relationship between laminar quantitative T_2^* and cortical thickness in multiple sclerosis. Although the clinical relevance of cortical tissue loss assessment in multiple sclerosis has been consistently reported in cross-sectional and longitudinal studies, the underlying mechanisms are still unknown (Geurts *et al.*, 2012). Cortical thinning may be the consequence of axonal transection by white matter lesions leading to neuronal loss or may underlie a degenerative process that primarily targets the cortical grey matter. The knowledge of the relationship between subpial demyelination and cortical atrophy has been hampered by the lack of tools able to image *in vivo* subpial pathology. In our multiple sclerosis cohort, longer

quantitative T_2^*, at all three depths, was associated with cortical thinning across several cortical areas. However, a clear preferential distribution through the cortical width in the correlation between these two measures was not evident, and in multiple sclerosis subjects changes in laminar quantitative T_2^* relative to controls were independent of cortical thickness. Although cortical thickness and normalized cortical volume were globally decreased in the cohort of subjects with multiple sclerosis relative to controls, and significant cortical thinning was also observed in SPMS cases, we did not find regional differences in cortical thickness between patients and controls. We calculated that for the patients with early and RRMS to have 80% power to detect a patient versus control difference in cortical thickness (which is ~80% of the standard deviation) at 5% significance, ~26 subjects per group would be necessary.

We did not find any correlation between cortical thickness or normalized cortical volume and either EDSS or MSSS; rather, quantitative T_2^* proved to be a marker of neurological disability more sensitive than cortical tissue loss. This suggests that taking into account the spatial variation of tissue integrity measures in the cortex can greatly improve the ability to find multiple sclerosis-related pathological changes. Laminar quantitative T_2^* and cortical thickness may also reflect distinctive aspects of a degenerative process that targets the cortex, and as such different measures of clinical disability. Pathological data indeed suggested that neuronal and axonal loss seem to contribute more than demyelination to cortical atrophy in multiple sclerosis (Klaver *et al.*, 2013). Longitudinal studies could help to elucidate the spatiotemporal events leading to cortical tissue loss in multiple sclerosis, as well as the contribution of white matter lesions.

Origin of cortical quantitative T_2^* changes in multiple sclerosis

In this study we detected an overall increase in quantitative T_2^* in patients, at all disease stages, relative to controls. Cortical T_2^* contrast has been associated predominantly with non-heme iron (Haacke *et al.*, 2005; Fukunaga *et al.*, 2010), which is stored in ferritin particles and provides a substrate for oligodendrocytes for producing and sustaining myelin sheaths surrounding axons. In healthy cortical laminae non-heme iron has been shown to co-localize with myelin on cellular and molecular levels (Connor and Menzies, 1990). In multiple sclerosis, in both white matter and cortical multiple sclerosis lesions longer T_2^* (or shorter R_2^*) has been pathologically related to iron and myelin loss (Yao *et al.*, 2012, 2014). Other histopathological–magnetic resonance correlations of *ex vivo* multiple sclerosis brains using gradient echo T_2^*-weighted imaging at 7 T found increased T_2^* signal in demyelinating lesions, and decreased T_2^* in focal areas characterized by the presence of iron rich microglia and/or macrophages (Pitt *et al.*, 2010). Findings from our study,

thus, likely reflect the prevailing effects of a pathological process that underlies a decrease in iron and/or myelin content rather than changes due to iron accumulation in the cortex.

In our multiple sclerosis cohort, quantitative T_2* measured in focal cortical lesions was significantly increased (longer T_2*) compared with NACGM quantitative T_2* and mean cortical quantitative T_2* in healthy controls, suggesting that focal cortical lesions may contribute, at least in part, to the observed changes in laminar quantitative T_2* in multiple sclerosis. Pathological–magnetic resonance correlations on gradient echo images at 7 T highlighted, however, that a consistent subset of cortical lesions can be missed at prospective visual inspection of magnetic resonance scans as cortical lesion counts greatly improved with retrospective scoring (i.e. after comparison of histological sections) (Pitt *et al.*, 2010; Yao *et al.*, 2014). Indeed in our study, in SPMS cases, quantitative T_2* changes relative to healthy controls also involved the NACGM. We previously reported in another multiple sclerosis cohort that in some patients, FLASH-T_2* magnitude images were characterized, in addition to focal subpial lesions, by the presence of diffuse band-like areas of subtle hyperintensity mainly involving the outer cortical laminae and extending over an entire gyrus or multiple gyri (Mainero *et al.*, 2009). These observations suggest that even at ultra-high field MRI visual characterization of focal cortical lesions does not account for the full spectrum of cortical pathology in multiple sclerosis, and that quantitative methods able to assess cortical damage voxel-wise could better depict the extent and pattern of cortical pathological changes in the disease.

Heme-bound iron, which may underlie normal vascularization, can also affect T_2* contrast. The contribution of intracortical vascular changes to cortical demyelination in multiple sclerosis, however, is still uncertain. Autopsy studies of late stage multiple sclerosis showed that cortical lesions lack the blood–brain barrier breakdown that characterizes active white matter lesions (Peterson *et al.*, 2001; Bo *et al.*, 2003*a*). Other histopathological examinations found blood–brain barrier breakdown and perivascular inflammation in the cortex of multiple sclerosis brains at disease onset (Lucchinetti *et al.*, 2011). *In vivo* assessments described a significant reduction in cerebral blood flow and cerebral blood volume in cortical lesions compared with the normal-appearing grey matter, suggesting reduced metabolism due to loss of cortical neurons. A subset of cortical lesions showing an increased cerebral blood flow and/or cerebral blood volume, however, was also detected, possibly implying that perfusion could evolve during inflammation (Peruzzo *et al.*, 2013). Other studies found, in early RRMS, decreased grey matter perfusion in the absence of volume loss, consistent with neuronal metabolic dysfunction (Debernard *et al.*, 2014). Preliminary findings using gadolinium-enhanced T_2-fluid-attenuated-inversion-recovery (FLAIR) MRI reported, in a subset of multiple sclerosis cases, leptomeningeal contrast enhancement that was unrelated to contrast-enhancement in white matter

lesions (Reich *et al.*, 2014). Taken together, these observations lead to speculation that the time course of cortical blood–brain barrier breakdown could differ from that in white matter lesions and across disease stages. Future studies aimed at assessing intracortical vascular changes in multiple sclerosis could help to clarify its role in cortical pathology. In addition, quantitative T_2* measurements can be combined with other techniques specific to myelin such as T_1 mapping, quantitative magnetization transfer imaging (Dortch *et al.*, 2013), and to iron such as quantitative suceptibility mapping (Deistung *et al.*, 2013) to better characterize the contribution of myelin and iron to cortical multiple sclerosis pathology.

Conclusion

This study demonstrates that a surface-based analysis of ultra-high resolution quantitative T_2* MRI acquisition at 7 T with a highly parallelized radiofrequency coil can facilitate the *in vivo* characterization of cortical pathology at distinct depths from the pial surface in multiple sclerosis. We were able to detect *in vivo* a gradient in the expression of intracortical multiple sclerosis pathology across disease stages, which supports the hypothesis that cortical pathology in multiple sclerosis may be, at least in part, the consequence of a pathogenic process driven from the pial surface. Because we cannot exclude that changes in deeper cortical laminae (75% depth) could also be driven by white matter lesions extending into the cortex, longitudinal evaluations are needed to confirm our preliminary observations. Nevertheless, the significant association between laminar quantitative T_2*, neurological disability and disease severity, prominent in the outer cortical layers and independent from white matter lesions, provides *in vivo* evidence that this pattern of cortical disease can be the pathological basis for disease progression in many multiple sclerosis cases.

Funding

Supplementary material

Supplementary material is available at *Brain* online.

References

Bagnato F, Hametner S, Yao B, van Gelderen P, Merkle H, Cantor FK, et al. Tracking iron in multiple sclerosis: a combined imaging and histopathological study at 7 Tesla. Brain 2011; 134 (Pt 12): 3602–15.

Bo L, Geurts JJ, van der Valk P, Polman C, Barkhof F. Lack of correlation between cortical demyelination and white matter pathologic changes in multiple sclerosis. Arch Neurol 2007; 64: 76–80.

Bo L, Vedeler CA, Nyland H, Trapp BD, Mork SJ. Intracortical multiple sclerosis lesions are not associated with increased lymphocyte infiltration. Mult Scler 2003a; 9: 323–31.

Bo L, Vedeler CA, Nyland HI, Trapp BD, Mork SJ. Subpial demyelination in the cerebral cortex of multiple sclerosis patients. J Neuropathol Exp Neurol 2003b; 62: 723–32.

Cohen-Adad J, Benner T, Greve D, Kinkel RP, Radding A, Fischl B, et al. *In vivo* evidence of disseminated subpial T2* signal changes in multiple sclerosis at 7T: a surface-based analysis. Neuroimage 2011; 57: 55–62.

Cohen-Adad J, Polimeni JR, Helmer KG, Benner T, McNab JA, Wald LL, et al. T2* mapping and B0 orientation-dependence at 7 T reveal cyto- and myeloarchitecture organization of the human cortex. Neuroimage 2012; 60: 1006–14.

Connor JR, Menzies SL. Altered cellular distribution of iron in the central nervous system of myelin deficient rats. Neuroscience 1990; 34: 265–71.

Dale AM, Fischl B, Sereno MI. Cortical surface-based analysis. I. Segmentation and surface reconstruction. Neuroimage 1999; 9: 179–94.

Debernard L, Melzer TR, Van Stockum S, Graham C, Wheeler-Kingshott CA, Dalrymple-Alford JC, et al. Reduced grey matter perfusion without volume loss in early relapsing-remitting multiple sclerosis. J Neurol Neurosurg Psychiatr 2014; 85: 544–51.

Deistung A, Schafer A, Schweser F, Biedermann U, Turner R, Reichenbach JR. Toward *in vivo* histology: a comparison of quantitative susceptibility mapping (QSM) with magnitude-, phase-, and R2*-imaging at ultra-high magnetic field strength. NeuroImage 2013; 65: 299–314.

Derakhshan M, Caramanos Z, Narayanan S, Arnold DL, Louis Collins D. Surface-based analysis reveals regions of reduced cortical magnetization transfer ratio in patients with multiple sclerosis: a proposed method for imaging subpial demyelination. Hum Brain Mapp 2014; 7: 3402–13.

Dortch RD, Moore J, Li K, Jankiewicz M, Gochberg DF, Hirtle JA, et al. Quantitative magnetization transfer imaging of human brain at 7 T. NeuroImage 2013; 64: 640–9.

Filippi M, Evangelou N, Kangarlu A, Inglese M, Mainero C, Horsfield MA, et al. Ultra-high-field MR imaging in multiple sclerosis. J Neurol Neurosurg Psychiatr 2014; 85: 60–6.

Fischl B, Dale AM. Measuring the thickness of the human cerebral cortex from magnetic resonance images. Proc Natl Acad Sci USA 2000; 97: 11050–5.

Fukunaga M, Li TQ, van Gelderen P, de Zwart JA, Shmueli K, Yao B, et al. Layer-specific variation of iron content in cerebral cortex as a source of MRI contrast. Proc Natl Acad Sci USA 2010; 107: 3834–9.

Geurts JJ, Calabrese M, Fisher E, Rudick RA. Measurement and clinical effect of grey matter pathology in multiple sclerosis. Lancet Neurol 2012; 11: 1082–92.

Govindarajan ST, Cohen-Adad J, Sormani MP, Fan AP, Louapre C, Mainero C. Reproducibility of T2* mapping in the human cerebral cortex *in vivo* at 7 Tesla MRI. J Magn Reson Imaging 2014. Advance Access published on November 19, 2014, doi: 10.1002/jmri.24789.

Greve DN, Fischl B. Accurate and robust brain image alignment using boundary-based registration. Neuroimage 2009; 48: 63–72.

Haacke EM, Cheng NY, House MJ, Liu Q, Neelavalli J, Ogg RJ, et al. Imaging iron stores in the brain using magnetic resonance imaging. Magnetic resonance imaging 2005; 23: 1–25.

Hagler DJ Jr, Saygin AP, Sereno MI. Smoothing and cluster thresholding for cortical surface-based group analysis of fMRI data. Neuroimage 2006; 33: 1093–103.

Howell OW, Reeves CA, Nicholas R, Carassiti D, Radotra B, Gentleman SM, et al. Meningeal inflammation is widespread and linked to cortical pathology in multiple sclerosis. Brain 2011; 134 (Pt 9): 2755–71.

Klaver R, De Vries HE, Schenk GJ, Geurts JJ. Grey matter damage in multiple sclerosis: a pathology perspective. Prion 2013; 7: 66–75.

Kurtzke JF. Rating neurologic impairment in multiple sclerosis: an expanded disability status scale (EDSS). Neurology 1983; 33: 1444–52.

Kutzelnigg A, Lassmann H. Cortical demyelination in multiple sclerosis: a substrate for cognitive deficits? J Neurol Sci 2006; 245: 123–6.

Langkammer C, Krebs N, Goessler W, Scheurer E, Ebner F, Yen K, et al. Quantitative MR imaging of brain iron: a postmortem validation study. Radiology 2010; 257: 455–62.

Lassmann H, Lucchinetti CF. Cortical demyelination in CNS inflammatory demyelinating diseases. Neurology 2008; 70: 332–3.

Li W, Wu B, Liu C. Quantitative susceptibility mapping of human brain reflects spatial variation in tissue composition. NeuroImage 2011; 55: 1645–56.

Lublin FD, Reingold SC. Defining the clinical course of multiple sclerosis: results of an international survey. National multiple sclerosis society (USA) advisory committee on clinical trials of new agents in multiple sclerosis. Neurology 1996; 46: 907–11.

Lublin FD. New multiple sclerosis phenotypic classification. Eur Neurol 2014; ; 72 ((Suppl 1): 1–5.

Lucchinetti CF, Popescu BF, Bunyan RF, Moll NM, Roemer SF, Lassmann H, et al. Inflammatory cortical demyelination in early multiple sclerosis. N Engl J Med 2011; 365: 2188–97.

Magliozzi R, Howell O, Vora A, Serafini B, Nicholas R, Puopolo M, et al. Meningeal B-cell follicles in secondary progressive multiple sclerosis associate with early onset of disease and severe cortical pathology. Brain 2007; 130 (Pt 4): 1089–104.

Magliozzi R, Howell OW, Reeves C, Roncaroli F, Nicholas R, Serafini B, et al. A Gradient of neuronal loss and meningeal inflammation in multiple sclerosis. Ann Neurol 2010; 68: 477–93.

Mainero C, Benner T, Radding A, van der Kouwe A, Jensen R, Rosen BR, et al. *In vivo* imaging of cortical pathology in multiple sclerosis using ultra-high field MRI. Neurology 2009; 73: 941–8.

McDonald WI, Compston A, Edan G, Goodkin D, Hartung HP, Lublin FD, et al. Recommended diagnostic criteria for multiple sclerosis: guidelines from the International Panel on the diagnosis of multiple sclerosis. Ann Neurol 2001; 50: 121–7.

Nielsen AS, Kinkel RP, Madigan N, Tinelli E, Benner T, Mainero C. Contribution of cortical lesion subtypes at 7T MRI to physical and cognitive performance in MS. Neurology 2013; 81: 641–9.

Peruzzo D, Castellaro M, Calabrese M, Veronese E, Rinaldi F, Bernardi V, et al. Heterogeneity of cortical lesions in multiple sclerosis: an MRI perfusion study. J Cereb Blood Flow Metab 2013; 33: 457–63.

Peterson JW, Bo L, Mork S, Chang A, Trapp BD. Transected neurites, apoptotic neurons, and reduced inflammation in cortical multiple sclerosis lesions. Ann Neurol 2001; 50: 389–400.

Pitt D, Boster A, Pei W, Wohleb E, Jasne A, Zachariah CR, et al. Imaging cortical lesions in multiple sclerosis with ultra-high-field magnetic resonance imaging. Arch Neurol 2010; 67: 812–8.

Reich D, Rao A, Vuolo L, Absinta M, Nair G, Butman J, et al. Leptomeningeal contrast enhancement: a possible marker of inflammation in the subarachnoid space. Proc Am Acad Neurol 2014.

Reynolds R, Roncaroli F, Nicholas R, Radotra B, Gveric D, Howell O. The neuropathological basis of clinical progression in multiple sclerosis. Acta Neuropathologica 2011; 122: 155–70.

Roxburgh RH, Seaman SR, Masterman T, Hensiek AE, Sawcer SJ, Vukusic S, et al. Multiple sclerosis severity score: using disability and disease duration to rate disease severity. Neurology 2005; 64: 1144–51.

Samson RS, Muhlert N, Sethi V, Wheeler-Kingshott CAM, Ron MA, Miller DH, et al. Sulcal and gyral crown cortical grey matter involvement in multiple sclerosis: a magnetisation transfer ratio study. Mult Scler Relat Disord 2013; 2: 204–12.

Samson RS, Cardoso MJ, Muhlert N, Sethi V, Wheeler-Kingshott CA, Ron M, et al. Investigation of outer cortical magnetisation transfer ratio abnormalities in multiple sclerosis clinical subgroups. Mult Scler 2014; 20: 1322–30.

Seewann A, Vrenken H, Kooi EJ, van der Valk P, Knol DL, Polman CH, et al. Imaging the tip of the iceberg: visualization of cortical lesions in multiple sclerosis. Mult Scler 2011; 17: 1202–10.

Waehnert MD, Dinse J, Weiss M, Streicher MN, Waehnert P, Geyer S, et al. Anatomically motivated modeling of cortical laminae. Neuroimage 2014; 93 (Pt 2): 210–20.

Yao B, Bagnato F, Matsuura E, Merkle H, van Gelderen P, Cantor FK, et al. Chronic multiple sclerosis lesions: characterization with high-field-strength MR imaging. Radiology 2012; 262: 206–15.

Yao B, Hametner S, van Gelderen P, Merkle H, Chen C, Lassmann H, et al. 7 tesla magnetic resonance imaging to detect cortical pathology in multiple sclerosis. PloS One 2014; 9: e108863.